Earth Planets Space, **65**, 139–148, 2013

Light scattering by cometary dust: Large-particle contribution

Evgenij Zubko[1,2]

[1]*Department of Physics, P.O. Box 64, FIN-00014, University of Helsinki, Finland*
[2]*Astronomical Institute of Kharkov National University, 35 Sumskaya St., Kharkov, 61022, Ukraine*

(Received January 11, 2012; Revised February 12, 2012; Accepted February 13, 2012; Online published March 12, 2013)

Using the discrete dipole approximation (DDA) and a model of agglomerated debris particles, we study the contribution of large particles on the light scattering by cometary dust. The numerical simulations show that moderately and highly absorbing particles larger than 3 μm do not significantly affect the backscattering phenomena observed at visible wavelengths in comets at phase angles $\alpha \leq 30^\circ$, such as the brightness surge and the negative polarization branch. Weakly and non-absorbing particles may play some role even if they are larger than 3 μm; but they are not abundant species in comets. However, the contribution of large particles on polarizations at phase angles $\alpha > 30^\circ$ can be significant, even though they are highly absorbing; simultaneously, the phase dependence of brightness remains insensitive to the contribution of large particles.

Key words: Comets, backscattering, enhancement of brightness, negative polarization, discrete dipole approximation.

1. Introduction

Photometry of comets at small phase angles $\alpha < 30^\circ$ shows an enhancement of their brightness with α decreasing toward 0° (e.g., Kiselev and Chernova, 1981; Meech and Jewitt, 1987; Joshi *et al.*, 2011). In the same range of α, polarimetry reveals generally negative values for the degree of linear polarization; therefore, this phenomenon is often referred to as *negative polarization* (e.g., Chernova *et al.*, 1993; Levasseur-Regourd *et al.*, 1996). Note that the degree of linear polarization is defined as follows: $P = (I_\perp - I_\parallel)/(I_\perp + I_\parallel)$, where, $I_\perp$ and $I_\parallel$ are the intensities of electromagnetic radiation vibrating perpendicular to and in the scattering plane respectively. Thus, *negative polarization* implies $I_\parallel > I_\perp$. The degree of linear polarization in comets is substantially positive at $\alpha > 30^\circ$.

Analysis of photometric observations of comets is a complicated problem due to their sporadic activity. In the range of small phase angles $\alpha < 30^\circ$, the brightness linearly increases as α decreases (Meech and Jewitt, 1987; Joshi *et al.*, 2011). Thus, comets do not produce a *photometric opposition effect*, i.e., a non-linear decrease of apparent magnitude near backscattering. Note that the opposition effect is a distinctive feature for asteroids of various types (e.g., Belskaya and Shevchenko, 2000). This phenomenon also appears in C-type dark asteroids; however, the angular profile of intensity becomes non-linear only at extremely small phase angles $\alpha < 2$–3°. For larger α, comets and dark asteroids have similar photometric behavior (Meech and Jewitt, 1987).

Interestingly, the full angular profile of the negative polarization in comets nearly coincides with that of dark C-type asteroids (e.g., Chernova *et al.*, 1993); i.e., it has a parabolic shape with a minimum of polarization $P_{\min} \approx -1.7\%$ that is located at phase angle $\alpha_{\min} = 10$–11°. Such resemblance has been interpreted to mean the objects have similar physical properties of dust particles in these two dramatically different objects (e.g., Myers and Nordsieck, 1984; Joshi *et al.*, 2003). However, the degree of linear polarization dramatically varies throughout the cometary coma. Specific features in the coma, such as jets and the circumnuclear halo have remarkably different polarizing properties that are different from the rest of the comet (e.g., Hadamcik and Levasseur-Regourd, 2003). It is only when averaging all these different regions that the polarization properties of comets and C-type asteroids are similar; therefore, this similarity appears to be coincidental (Zubko, 2011).

Photo-polarimetry can provide clues to the physical properties of dust in comets. For instance, the negative polarization has a strong dependence on absorption of dust particle material; whereas, the appearance of this polarimetric feature itself constrains the imaginary part of the refractive index Im(m) from being not higher than approximately 0.1 (Zubko *et al.*, 2009; Zubko, 2011). Therefore, when observing variations of the negative polarization throughout cometary coma, one can discriminate areas with high concentration of weakly absorbing Mg-rich silicates or highly absorbing carbonaceous materials. These two materials are known to be highly abundant species within comets (e.g., Fomenkova, 1999; Jessberger, 1999).

An important question that, to our knowledge, has not been rigorously addressed in the literature so far, concerns the contribution of large grains on the light scattering by cometary dust. This research was designed to fill this gap, and we carry out a quantitative investigation on the relative

doi:10.5047/eps.2012.02.003

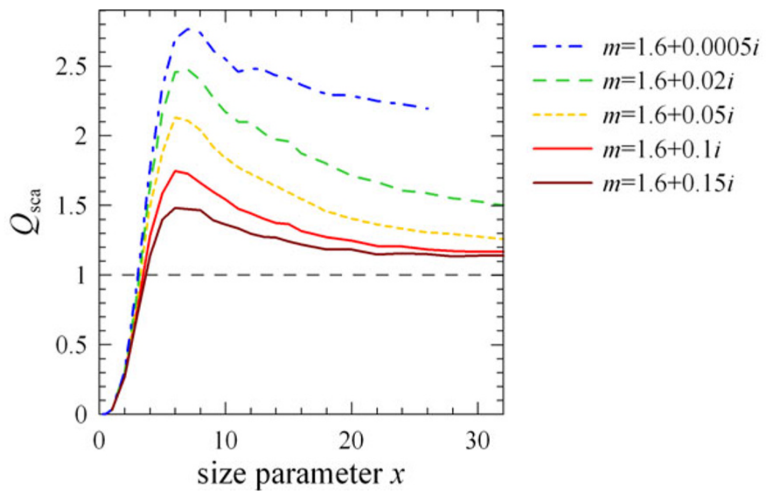

Fig. 1. Scattering efficiency $Q_{\rm sca}$ as function of size parameter x of agglomerated debris particles having different material absorption.

contribution of dust grains with sizes larger than approximately 3 μm on the light scattered from comets. Though this chosen specification of large particles does seem to be random, as will be shown latter in Section 3, it has a significant practical consequence for fast, realistic numerical simulations of light scattering by cometary dust.

2. Size Distribution of Cometary Dust and Contribution of Dust Particles with Different Sizes on the Scattered Light

In situ measurements of comet 1P/Halley with *VeGa-1* and *2* spacecrafts revealed that the dust particles span the range of mass from at least 10^{-16} to 10^{-6} g (Mazets *et al.*, 1986). Taking into account the material density of cometary dust being 0.3–3 g/cm^3 (e.g., Hörz *et al.*, 2006), one can see that the size of dust particles spans five orders of magnitude from 10^{-2} to 10^2 μm. However, it is expected that the size of dust grains in comets exceed this upper limit of one hundred microns. Cometary dust was found to obey the power-law size distribution r^{-a}, where r is the radius of the particle and the power index a varies with the mass of the dust particles from 1.5 (in the case of 10^{-16} g) to 3.4 (for 10^{-6} g) (Mazets *et al.*, 1986). Such a size distribution implies that the number of smaller grains significantly dominates over that of larger ones.

The relative contribution of dust particles on the photo-polarimetric properties of comets depends upon not only their number density but also on their scattering efficiencies, which depend on the ratio of the particle size to the wavelength λ of the incident light. This ratio often is quantified by the so-called *size parameter* x, which is defined as $x = 2\pi r/\lambda$ (e.g., Bohren and Huffman, 1983). For irregular particles, we attribute radius r to a sphere circumscribing the target particle.

If the particle is much smaller than the wavelength of the incident light λ (i.e., $x \ll 1$; for spherical particles, this case is referred to as *Rayleigh scattering*), the intensity of the scattered light depends on particle radius as r^6 (e.g., Bohren and Huffman, 1983). In practice, this means that a decrease of size by 2 times makes the light scattered by the particle dimmer by 64 times. Even though, due to the size distribution $r^{-3.5}$, the number of half-sized particles may be about 11 times greater, it is evident that this greater number density cannot compensate for the overall decrease of intensity of their scattered light. As a consequence, the contribution of dust particles, which are significantly smaller than λ, becomes inconsequential to the total signal.

The situation changes dramatically as the radius of the target particle approaches the wavelength, i.e., x becomes greater than 5–6. In order to give a quantitative assessment of this phenomenon, we analyze the size dependence of the scattering efficiency $Q_{\rm sca}$, which is dimensionless and defined as the ratio of the scattering cross section $C_{\rm sca}$ divided by the geometric cross section G of the target particles (e.g., Bohren and Huffman, 1983). When $Q_{\rm sca} = 1$, the particle scatters the same amount of electromagnetic energy flux that flows through its geometric cross section. However, particles whose sizes are comparable with the wavelength have scattering efficiencies that can significantly exceed 1, making such particles extremely efficient at light scattering. This is true for all particle morphologies. For instance, Fig. 1 shows scattering efficiencies as a function of size parameter x of model agglomerated debris particles (shown in Fig. 2) that were constructed to analyze photo-polarimetric observations of comets (e.g., Zubko *et al.*, 2009, 2011a; Zubko, 2011). In all cases, the scattering efficiency has a maximum at $x \sim 6$–7. For weakly absorbing particles (e.g., $m = 1.6 + 0.0005i$), the scattering efficiency $Q_{\rm sca}$ is as high as ~2.8. Though an increase of the imaginary part of the refractive index Im(m) substantially decreases this maximum amplitude, $Q_{\rm sca}$ remains greater than 1. As particle size is increased further, e.g. $x > 7$, $Q_{\rm sca}$ clearly decreases. This behavior is similar for irregular particles having quite different morphologies (Zubko, 2012). However, it implies that, in the range of x from 7 up to 20, the relative contribution of dust particles on the light scattering gets weaker not only due to smaller number density but, also, because of their poor efficiency for scattering. As a consequence, one could expect a leading role for particles with sizes comparable to wavelength in light scattering by polydisperse cometary dust.

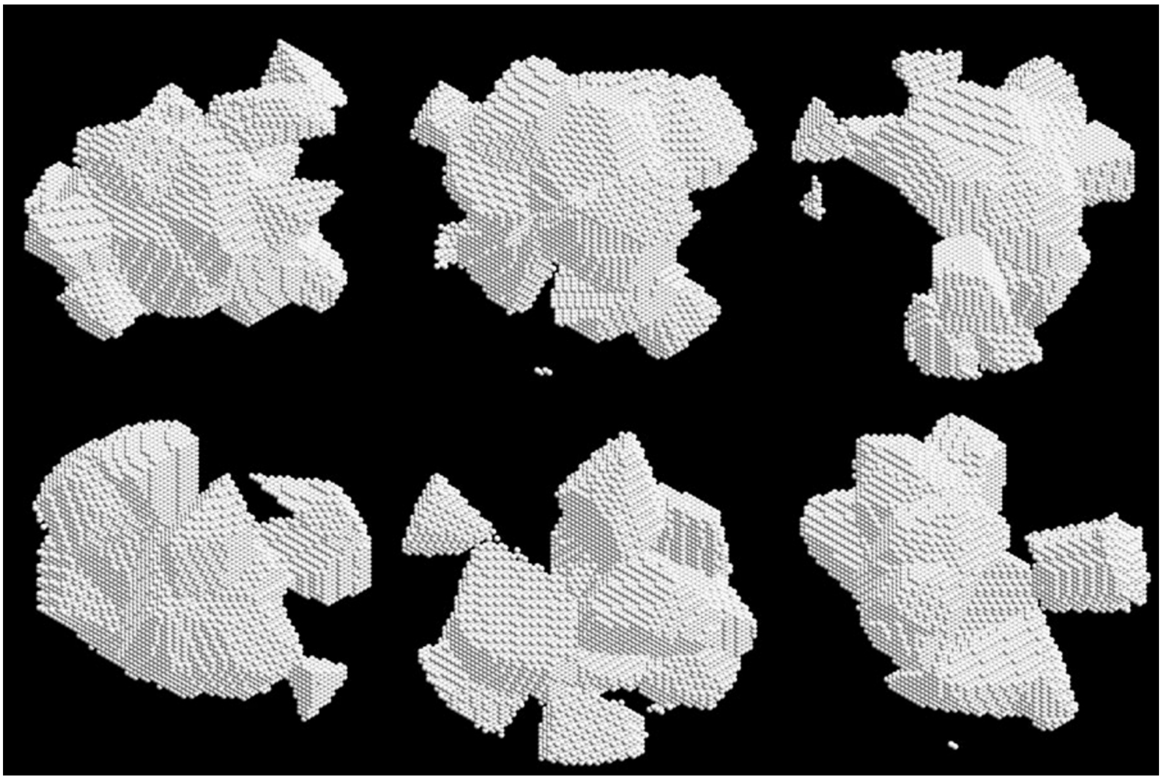

Fig. 2. Examples of agglomerated debris particles.

3. Numerical Simulation of Light Scattering by Irregularly Shaped Particles

In order to give a quantitative assessment of the speculations presented in Section 2, we compute light scattering by polydisperse agglomerated debris particles using the DDA (e.g., Zubko *et al.*, 2010; and references therein). In the DDA, a target is modeled with an array of small constituent volumes that together reproduce the shape and internal optical properties of the original particles. These constituent volumes are chosen to be significantly smaller than the wavelength of the incident light. Under such condition, light scattering by these constituent volumes can be expressed analytically with the *Rayleigh approximation* (e.g., Bohren and Huffman, 1983). Owing to such a replacement, one can reduce the light-scattering problem to a system of linear algebraic equations. Note that we use our well-tested implementation of the DDA to perform the calculations of this manuscript (e.g., Zubko *et al.*, 2010).

An important parameter specifying the DDA applicability is the size of the cubic lattice d. In application to irregular particles, the DDA provides accurate numerical result under the condition $kd|m| \leq 1$ (Zubko *et al.*, 2010); where $k = 2\pi/\lambda$ is the wavenumber. Throughout this study, the parameter $kd|m|$ remains less than 0.85, giving an additional reliability for the numerical results.

One optional restriction on constituent volumes is that they are located in a regular cubic lattice to allow use of the fast Fourier transformation (FFT), which dramatically accelerates computations (Goodman *et al.*, 1991). In order to achieve a maximum gain in the FFT use, the size of the cubic lattice along each coordinate axis should take the form 2^L, where L is an integer. We use two sizes of cubic lattice, namely, $64 \times 64 \times 64$ and $128 \times 128 \times 128$ cells, depending on the target particle size. The computations in the larger cubic lattice are about 8 times slower and consume 8 times more memory than those of the smaller cubic lattice.

We generate agglomerated debris particles by starting with a perfect sphere and using the following algorithm. A spherical volume is filled with a regular cubic lattice that is considered as the initial matrix of the irregular particles. In a cubic lattice with a size of $64\times64\times64$ elements, the initial matrix consists of 137,376 cells; whereas, $128 \times 128 \times 128$ lattice contains 1,099,136 cells. All the cells forming this initial matrix are divided into two groups: cells belonging to the surface layer and cells internal to the surface layer. The surface layer is chosen to be thin: its depth is equal to 1% of the initial matrix radius. Among surface dipoles, we choose randomly 100 cells that are considered as seed cells of empty space. In the set of internal cells, we randomly choose 21 seed cells of material and 20 of empty space. Then, step-by-step, each cell distinct from the seed cells is marked with the same optical properties as that of the nearest seed cell. Sample images of the shapes generated with such algorithm are shown in Fig. 2.

The size of the irregular particles can be characterized by the size of the circumscribing sphere. In the case of agglomerated debris particles, this size nearly coincides with the size of the initial matrix. An extremely important parameter characterizing agglomerate particles is the packing density of their material ρ. This is defined as the ratio of particle volume over total volume of the circumscribing sphere and, for agglomerated debris particles, it is equal to 0.236. Note that the geometric cross section of agglomerated debris particles is equal to 0.61 of the projected area corresponding to the circumscribing sphere.

One important question is how the packing density of the model particles compares with that of cometary particles measured *in situ*. An analysis of the microcraters in the aluminum foil covering the *Stardust* sample collector reveals the material density of cometary dust particles being in the range 0.3–3 g/cm^3 (e.g., Hörz *et al.*, 2006). If we assume the bulk material density for refractory species in comets, i.e., organics and Mg-rich silicates (Fomenkova, 1999; Jessberger, 1999), is in the range 1.5–3.5 g/cm^3, one can estimate the material density in the agglomerated debris particles being in the range from 0.35 to 0.83 g/cm^3. These values are consistent with the *Stardust* findings. In application to comets, agglomerated debris particles would be classified as those having fluffy morphology.

We compute light scattering by agglomerated debris particles having five different refractive indices $m = 1.6 + 0.0005i$, $1.6+0.02i$, $1.6+0.05i$, $1.6+0.1i$, and $1.6+0.15i$. Weakly absorbing cases have an imaginary part of refractive index $\mathrm{Im}(m) \approx 0$ that is representative of Mg-rich silicates (e.g., Dorschner *et al.*, 1995); whereas, highly absorbing cases with $\mathrm{Im}(m) = 0.1$–0.15 can be attributed to organic materials (e.g., Khare *et al.*, 1990; Jenniskens, 1993). As was already mentioned, both are abundant species in comets. Note that, in the current paper, agglomerated debris particles are assumed to be homogenous, i.e., refractive index m does not vary throughout a particle volume. This is an approximation as cometary dust is chemically (and, therefore, optically) inhomogeneous (e.g., Fomenkova, 1999; Jessberger, 1999). However, the refractive index of homogenous agglomerated debris particles can be interpreted in terms of a complex refractive index for mixture of Mg-rich and organic materials. The real part of refractive index of Mg-rich silicates $\mathrm{Re}(m) \approx 1.6$ (Dorschner *et al.*, 1995) is somewhat similar to that is found in organic materials (Khare *et al.*, 1990; Jenniskens, 1993); whereas, imaginary part $\mathrm{Im}(m)$ differs dramatically, 0 versus 0.1–0.15. Therefore, the mixture of Mg-rich silicates and organic materials could yield a complex refractive indices like $m = 1.6 + 0.02i$ and $m = 1.6 + 0.05i$.

It is important to warn the reader from a direct comparison of the results for agglomerated debris particles presented below with photo-polarimetric observations of comets. In comets, we deal with a mixture of dust particles having completely different optical properties; whereas, in the given paper, we consider those constituents separately one from another. Furthermore, the considered list of the cometary materials is surely not a complete. For instance, organic materials reveal wide variety in their refractive index, depending upon circumstances of formation (e.g., Jenniskens, 1993). Moreover, if a comet was observed at heliocentric distances larger than 3 AU, one needs to take into consideration an abundance of water-ice particles; their refractive index is $m = 1.313 + 0i$, in visible.

For each refractive index, we consider a wide range of size parameter x of the agglomerated debris particles that varies from 1 to 32, except for the case of $m = 1.6 + 0.0005i$, when the upper limit is restricted to 26 due to DDA convergence limitations. In the range of $x = 1$–16, the increment of x is 1; whereas, for $x = 16$–$32(26)$, it is 2. We use a small initial matrix for the simulation of light scattering by particles with $x \leq 15$, otherwise a large initial matrix is used. For incident red light illumination with $\lambda = 0.633$ μm, the given range of x corresponds approximately to particles sizes from 0.2 μm to 6.5 μm (5.2 μm for $m = 1.6 + 0.0005i$); whereas, the threshold size parameter $x = 15$ represents particles with size of 3 μm.

Light-scattering properties of irregularly shaped particles are averaged over a minimum of 500 particle shapes. Light scattering by each sample particle is computed for only one random orientation of the incident electromagnetic wave, but we average the scattered field over 100 scattering planes, evenly distributed around the propagation direction of the incident light. Such averaging improves the statistical reliability of the numerical results, with minimal computational effort. The averaging is continued over additional sample particles until fluctuations of the standard deviation of the degree of linear polarization over the entire range of phase angle α is less than 1% (Zubko *et al.*, 2010). The actual number of sample particles considered for each set of parameters very often exceeds 500.

4. Results and Discussion

Obtaining statistically reliable numerical simulations of light scattering by cometary dust particles requires significant computational resources. These efforts are not evenly distributed throughout the particle sizes. For example, using four modern quad-core processors, the computation of the average light scattering by agglomerated debris particles with $m = 1.6 + 0.05i$ takes only approximately three days for the 15 smallest sizes in the range of $x = 1$–15; whereas, the other 9 sizes in the range of $x = 16$–32 require up to four weeks of calculations. Therefore, computational efforts are primarily applied to incorporate particles with sizes exceeding $x > 15$, which corresponds to particle sizes greater than 3 μm at $\lambda = 0.633$ μm. However, the specific size distribution of cometary dust together with an enhanced efficiency of particles comparable to wavelength discussed in Section 2, may make the contribution of particles larger than 3 μm relatively insignificant. If this is the case, then vast resources can be preserved by not performing these calculations for the larger particles.

This problem can be investigated using two polydisperse systems of agglomerated debris particles. One of them is formed by particles of all sizes available for the given refractive index, i.e., $x = 1$–32 (26), and the other one has a more limited range of sizes with $x = 1$–15. The extent of these size ranges differs by about a factor of two. A comparative analysis of the light scattering from these two systems allows us to evaluate the impact of large particles on the total light scattering.

We make this comparison for different values of the index a in the power-law size distribution r^{-a}. Figures 3–5 show results for $a = 1.5$, 2.5, and 3.5, respectively. These values of a are consistent with *in situ* measurements of cometary dust, which correspond to a wide range of particle mass from 10^{-16} to 10^{-6} g. Assuming the material density to be in the range from 0.35 to 0.83 g/cm^3, the mass of our model particles spans from 10^{-15} to 10^{-10} g. For such a

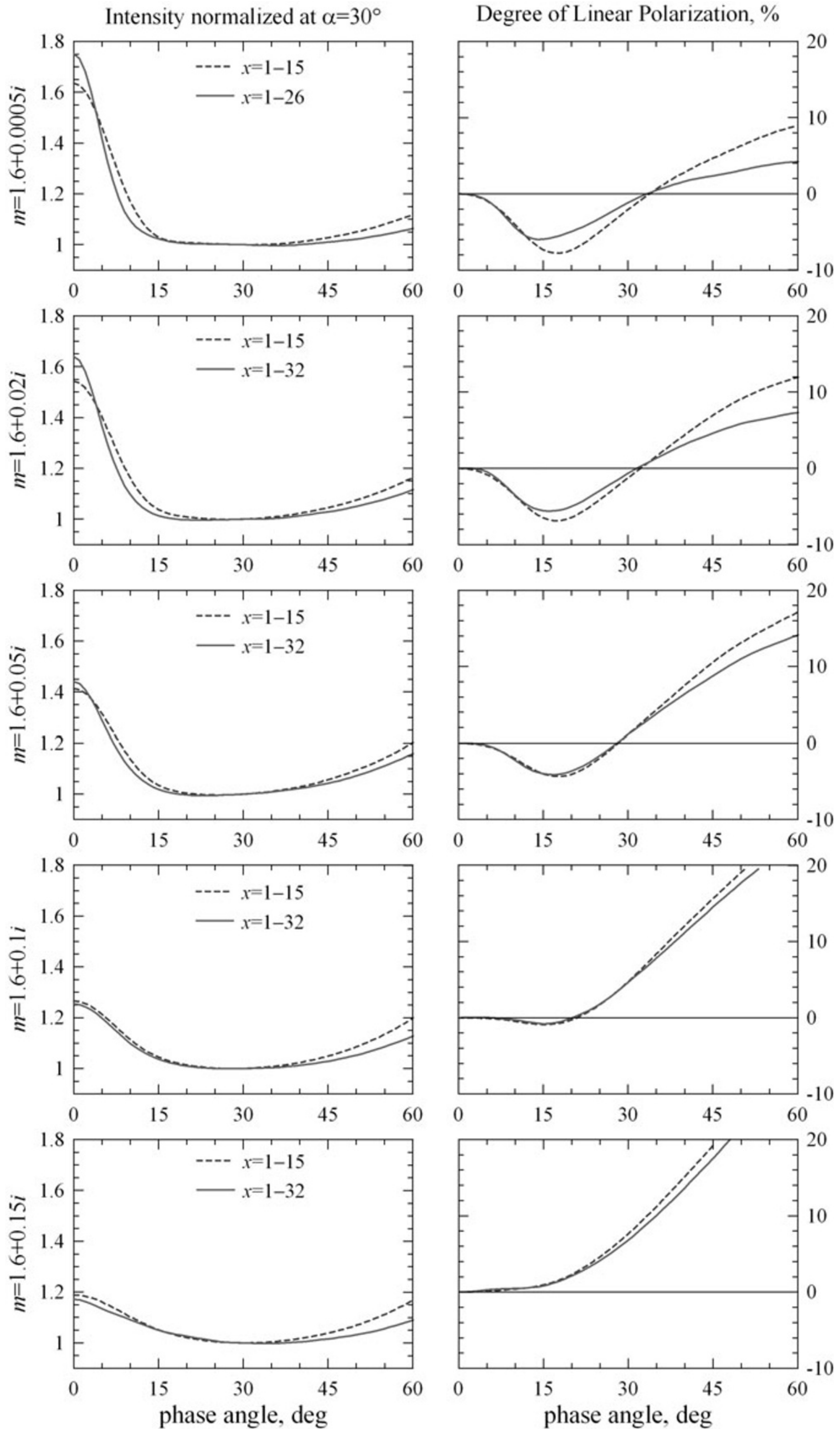

Fig. 3. Phase dependence of intensity I (left) and degree of linear polarization P (right) for agglomerated debris particles averaged over size and having a power-law size distribution with $a = 1.5$. The solid line corresponds to the case when particles of all available sizes are incorporated (x = 1–26, 32); whereas, the dashed line shows results only for small particles (x = 1–15). Each of the five different rows represents different material absorption spanning the range of the imaginary part of refractive index Im(m) from 0.0005 throughout 0.15.

mass range, *in situ* measurements yield the index $a = 1.5$–3 (Mazets *et al.*, 1986). Note also that the index a is not necessarily constant in comets. Polarimetric observations of comets suggest that the index a may be time-dependent and vary throughout the coma (e.g., Zubko *et al.*, 2011a).

Figures 3–5 show intensity (left) and degree of linear polarization (right) of the scattered light as function of phase angle α. We focus on the important range of phase angles α = 0–60°, where the backscattering phenomena are observed. Moreover, the vast majority of photo-polarimetric observations of comets reported in the scientific literature fall within this range of phase angle α. Note that the intensity is normalized to the middle phase angle $\alpha = 30°$. Each figure shows five rows of panels corresponding to refractive

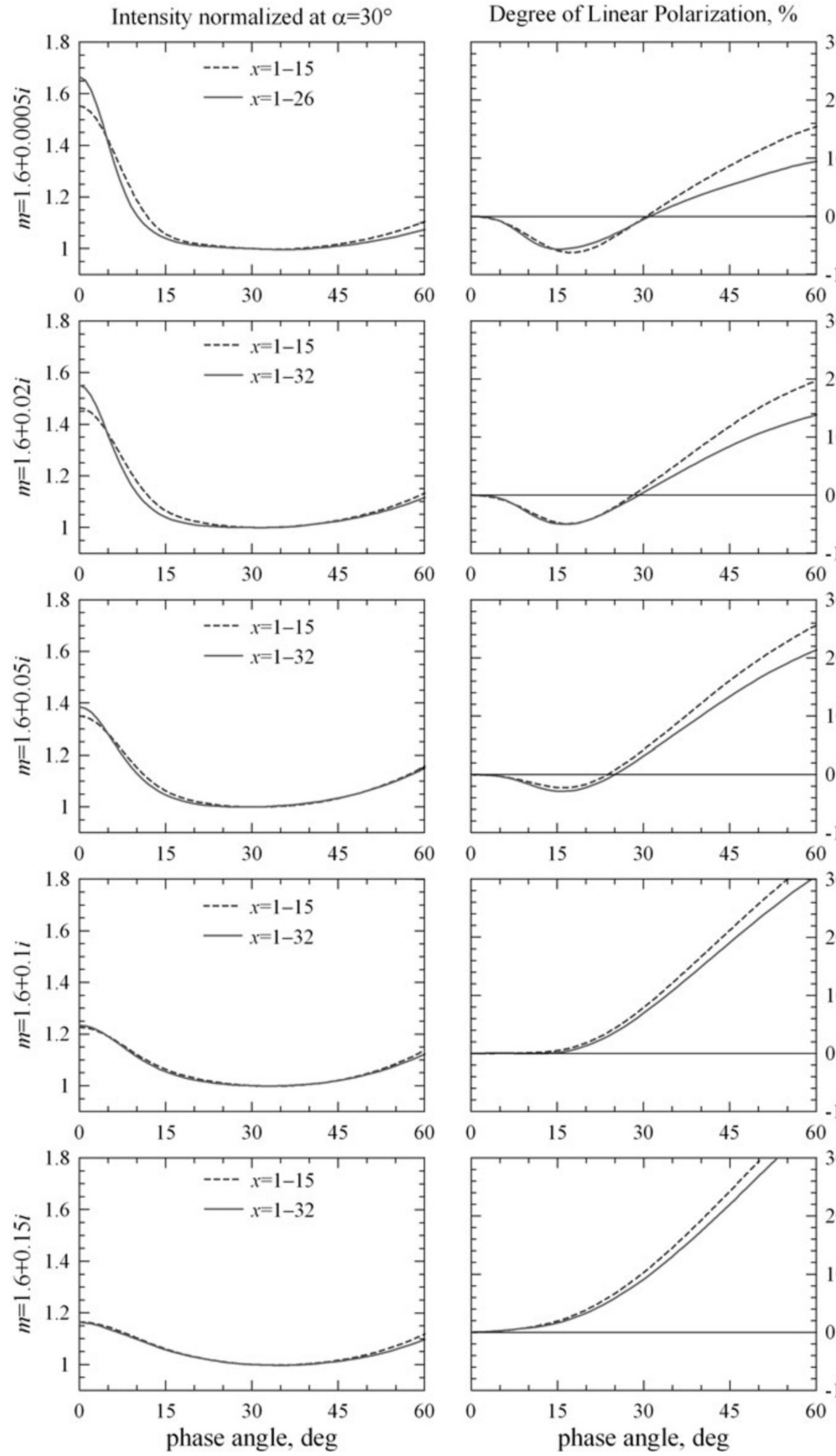

Fig. 4. Similar to Fig. 3 but for a power-law size-distribution index $a = 2.5$.

indices varying from $m = 1.6+0.0005i$ to $m = 1.6+0.15i$. Everywhere, the solid line corresponds to the case when the full size range is considered, and the dashed line corresponds to the truncated size range where the larger particles are not included.

As one can see in Fig. 3 ($a = 1.5$), the angular profiles of the light-scattering intensity from the full and the limited polydisperse systems are nearly coincident throughout the phase-angle range $\alpha = 5$–45°. However, for highly absorbing particles with $\mathrm{Im}(m) \geq 0.05$, this resemblance also extends to very small phase angles $\alpha = 0$–5°. Even in the case of weakly absorbing particles with $\mathrm{Im}(m) \leq 0.02$, the limited set of particles reproduces reasonably well the overall shape of the non-linear intensity surge at $\alpha < 20^\circ$. The divergence between the intensity curves for the full and limited polydisperse systems is much less than the short-term variations of cometary brightness (e.g., Meech and Jewitt, 1987; Joshi *et al.*, 2011). Owing to such variations, the de-

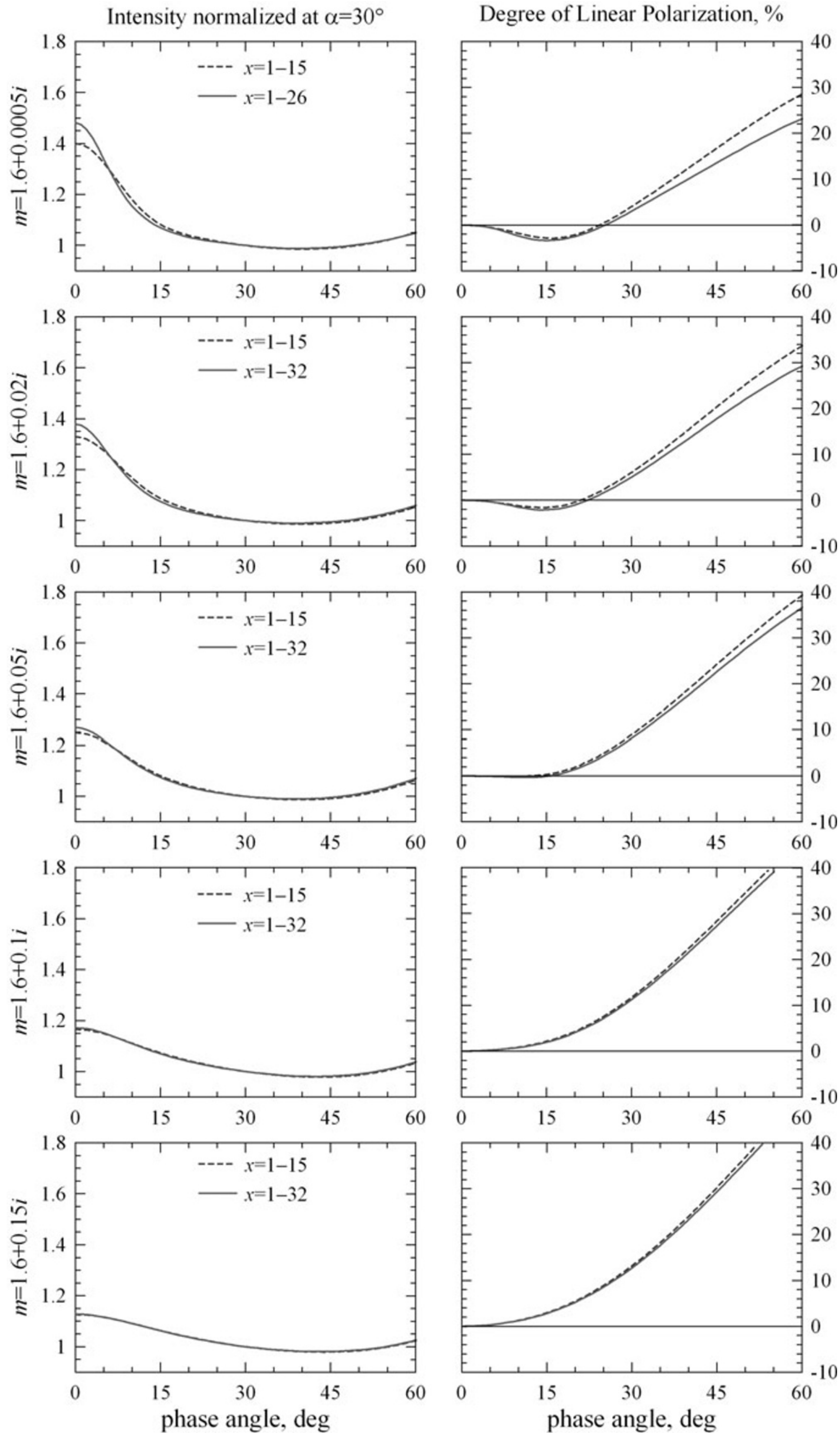

Fig. 5. Similar to Fig. 3 but for a power-law size-distribution index $a = 3.5$.

pendence of cometary brightness on phase angle is always obtained with considerable uncertainty. Therefore, the relatively small errors resulting from the elimination of the contribution of large particles would not affect significantly the interpretation of photometric observations of active comets.

Unlike intensity, the degree of linear polarization appears more sensitive to the contribution of large particles at $a = 1.5$. Indeed, the divergence of the polarization curves for the full and limited polydisperse systems at $m = 1.6 + 0.0005i$ confidently exceeds the accuracy of polarimetric observations, which is typically about 1%. The large particles reduce amplitude and, simultaneously, change the shape of the negative polarization branch, making it visibly asymmetric with the polarization minimum shifted toward $\alpha = 0°$. However, weakly absorbing particles do not dominate in the whole comet (e.g., Fomenkova, 1999), although they appear to dominate the signal in the innermost part of the coma (Zubko *et al.*, 2009; Zubko, 2011). An increase of

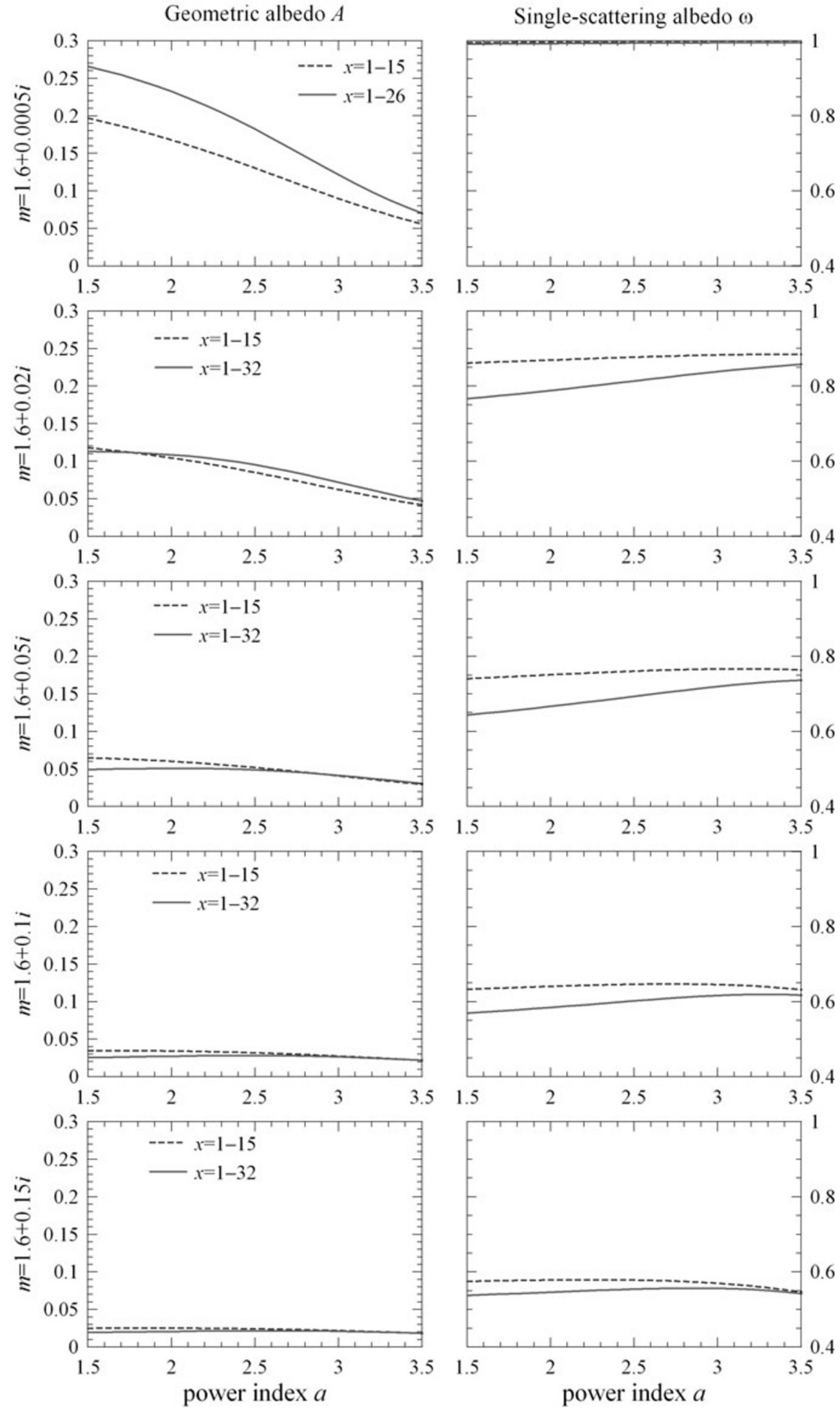

Fig. 6. Geometric albedo A (left) and single-scattering albedo ω (right) for agglomerated debris particles averaged over size as function of the index in power-law size distribution a. The solid line corresponds to the case when particles of all available sizes are incorporated (x = 1–26, 32), and the dashed line corresponds to results only for small particles (x = 1–15). The five different rows show the effect of material absorption.

the material absorption remarkably reduces the difference between the polarization curves. Nevertheless, for phase angles $\alpha > 30^\circ$, the errors are greater than observation errors (i.e., $\pm 1\%$). As follows from Fig. 3, an increase of Im(m) efficiently reduces the negative polarization branch and completely washes it out when Im(m) ≥ 0.1; this finding is consistent with the results of Zubko *et al.* (2009). The resemblance in polarization of the full and the limited systems at small phase angles $\alpha \leq 30^\circ$ appears regardless of whether the negative polarization phenomena are present.

Increasing the index a in the power-law size distribution r^{-a} increases the number density of small particles and, so, enhances their relative contribution. Therefore, one can expect that the difference in light scattering from the full and the limited polydisperse systems will be decreased as the index a increases. Such a trend is indeed observed through Fig. 3 ($a = 1.5$), Fig. 4 ($a = 2.5$), and Fig. 5 ($a = 3.5$). In particular, an increase of the index a from 1.5 to 2.5 (compare Figs. 3 and 4) already substantially improves the agreement between the angular profiles of intensity of light scattered from the full and the limited systems. At $\mathrm{Im}(m) \geq 0.05$, the curves are nearly coincident throughout all phase angles, i.e., $\alpha = 0$–$60°$. In the case of weakly absorbing particles with $\mathrm{Im}(m) \leq 0.02$, there remains a difference in the intensity curves at very small phase angles $\alpha < 5°$. Further increasing index a to 3.5 makes the agreement between the intensity curves even better as compared to $a = 2.5$ (compare Figs. 5 and 4).

As one can see from Figs. 3–5, the polarization curves of the full and the limited polydisperse systems become more similar as the index a increases. It especially holds for the range of small phase angles $\alpha \leq 30°$, where the curves are practically indistinguishable at $a = 2.5$ and 3.5 (see Figs. 4 and 5). At larger phase angles $\alpha > 30°$, an accurate numerical simulation of the degree of linear polarization in comets may require the inclusion of the large-particle contribution. This contribution is significant if the cometary dust consist primarily of weakly absorbing materials with $\mathrm{Im}(m) \leq 0.02$ and/or obey the power-law size distribution with the index $a \leq 2.5$. Though this may not be the case for the whole comet, these conditions may hold for some specific parts of the coma, like the innermost circumnuclear haloes (Zubko *et al.*, 2009, 2011a, b).

Two other important characteristics of cometary dust are the single-scattering and the geometric albedo. The single-scattering albedo ω is defined as a ratio of the scattering cross section C_{sca} over the extinction cross section C_{ext} (e.g., Bohren and Huffman, 1983). This quantifies the rate of energy of the incident radiation that is elastically scattered into the surrounding space. The single-scattering albedo takes values between 0 (an idealistic case of full absorption of the incident radiation) and 1 (full scattering). Unlike the single-scattering albedo ω, the geometric albedo A relates the intensity of light backscattered by a target to that by a white Lambert disk of the same geometric cross-section (e.g., Hanner, 2003). The geometric albedo A is defined as follows: $A = (S_{11}(0)\pi)/(k^2 G)$; where $S_{11}(0)$ is the element of Mueller matrix at $\alpha = 0°$ (e.g., Bohren and Huffman, 1983), and G is the geometric cross section of the target particle. It is important to stress that the geometric albedo A plays an important role as it helps to estimate the *dust production rate* of comets from their photometric observations in continuum (e.g., Newburn and Spinrad, 1989). Note that the *dust production rate* is equal to the mass of dust ejected from a comet per unit time. It is widely believed that cometary dust is quite dark in the visible and its average geometric albedo does not exceed 0.05 (e.g., Newburn and Spinrad, 1989; Hanner, 2003).

Figure 6 shows the geometric albedo A (left) and the single-scattering albedo ω (right) as functions of the index a in the power-law size distribution r^{-a}. When the absorption is not low, at $\mathrm{Im}(m) \geq 0.02$, there is very good quantitative agreement throughout the entire range of a between the two distributions, so the limited system provides adequate accuracy for the geometric albedo A. However, in the case of $m = 1.6 + 0.0005i$, the particles with $x > 15$ significantly affect the geometric albedo A, and their contribution is necessary.

The average geometric albedo in comets $A \approx 0.05$ could be immediately achieved with the agglomerated debris particles having $m = 1.6 + 0.02i$ and $1.6 + 0.05i$. The particles with $m = 1.6 + 0.0005i$ are too bright in appearance; whereas, particles with $m = 1.6 + 0.1i$ and $1.6 + 0.15i$ are up to a few times darker than average cometary dust. In our simulations, we consider homogeneous particles, but real cometary dust is substantially inhomogeneous by chemical composition and a realistic simulation of light scattering by comets must take into account this fact. Our understanding suggests that weakly absorbing Mg-rich silicates dominate in only about 25% of all dust particles and the rest of cometary particles consist of highly absorbing, primarily carbonaceous materials (e.g., Fomenkova, 1999; Jessberger, 1999). The mixture of these two types of particles may easily reproduce the average geometric albedo in comets. For instance, one particle with $A = 0.14$ and three dark particles with $A = 0.02$ yield an average geometric albedo $A = 0.05$, which is consistent with what is assumed for the whole comet. Nevertheless, taken independently, neither of those two components is consistent with the light-scattering properties of comets.

As one can see in Fig. 6, the single-scattering albedo ω of the full system can be quite well reproduced with the limited system at $m = 1.6 + 0.0005i$ and $1.6 + 0.15i$; whereas, the intermediate refractive indices may require the contribution of the large particles. However, agreement in ω is improved as the index a increases and, so, at $a \geq 3$, the limited polydisperse system may provide adequate accuracy. Note also that omitting the large particles systematically overestimates the single-scattering albedo. Thus, the data obtained for the limited system could be considered as an upper limit for ω.

5. Conclusion

Numerical simulation of light scattering by irregularly shaped particles shows that if the target particles obey a power-law size distribution similar to what has been observed for cometary dust, then the relative contribution of particles with $x > 15$ is generally weak and, therefore, in various realistic circumstances, it can be inconsequential. For instance, backscattering phenomena, such as the intensity surge and the negative polarization, as well as the geometric albedo A, can be accurately reproduced with particles limited to $x \leq 15$ when the target particles have moderate or high absorption material $\mathrm{Im}(m) \geq 0.02$. Moreover, even in the case of weakly absorbing particles $\mathrm{Im}(m) \approx 0$, one can obtain reliable results for backscattering phenomena if the power-law index a exceeds 2.5. Accurate computations of the geometric albedo A at $\mathrm{Im}(m) \approx 0$ requires the contribution of large particles with $x > 15$ throughout the entire range of the index $a = 1.5$–3.5.

Unlike within the backscattering regime, simulation of polarimetric properties of comets at non-small phase angles $\alpha > 30°$, in general, needs to include the contribution of large particles, except maybe for the cases of highly absorbing particles with $\mathrm{Im}(m) = 0.1$–0.15 when the index $a = 3.5$. It is interesting to note that in this same range of

α, the intensity is much less sensitive to the contribution of the large particles, so the photometric properties of comets can be reproduced with particles of the limited sizes.

An important practical outcome of the present work is that omitting particles with $x > 15$ dramatically speeds up the DDA computations. This feature substantially simplifies the numerical simulation of light scattering by cometary dust. Note that the threshold size parameter $x = 15$ corresponds to the size of dust particles being 3 μm in red light ($\lambda = 0.633$ μm) and 2 μm in blue light ($\lambda = 0.433$ μm). Our finding also is valid in the opposite sense: if the cometary dust particles consist of primarily highly absorbing materials, such as carbonaceous materials, then most of the visible light coming from comets is scattered by particles whose sizes are less than 3 μm. However, this does not exclude the possibility of the presence of a small fraction of weakly absorbing particles.

Acknowledgments. This research was partially supported by the Academy of Finland (contract 127461) and by the NASA program for Outer Planets Research (grant NNX10AP93G). I would like to thank Dr. Gorden Videen (Army Research Laboratory, USA), Prof. Karri Muinonen (University of Helsinki, Finland), and Prof. Yuriy Shkuratov (Kharkov National University, Ukraine) for their valuable comments on this work. I am also thankful to Prof. J. H. Hough and an anonymous reviewer for their constructive reviews.

References

Belskaya, I. N. and V. G. Shevchenko, Opposition effect of asteroids, *Icarus*, **147**, 94–105, 2000.

Bohren, C. F. and D. R. Huffman, *Absorption and Scattering of Light by Small Particles*, 530 pp., Wiley, New York, 1983.

Chernova, G. P., N. N. Kiselev, and K. Jockers, Polarimetric characteristics of dust particles as observed in 13 comets—Comparisons with asteroids, *Icarus*, **103**, 144–158, 1993.

Dorschner, J., B. Begemann, T. Henning, C. Jaeger, and H. Mutschke, Steps toward interstellar silicate mineralogy. II. Study of Mg-Fe-silicate glasses of variable composition, *Astron. Astrophys.*, **300**, 503–520, 1995.

Fomenkova, M. N., On the organic refractory component of cometary dust, *Space Sci. Rev.*, **90**, 109–114, 1999.

Goodman, J. J., B. T. Draine, and P. J. Flatau, Application of fast-Fourier-transform techniques to the discrete-dipole approximation, *Opt. Lett.*, **16**, 1198–1200, 1991.

Hadamcik, E. and A. C. Levasseur-Regourd, maging polarimetry of cometary dust: different comets and phase angles, *J. Quant. Spectr. Rad. Trans.*, **79–80**, 661–678, 2003.

Hanner, M. S., The scattering properties of cometary dust, *J. Quant. Spectr. Rad. Trans.*, **79–80**, 695–705, 2003.

Hörz, F., R. Bastien, J. Borg, J. P. Bradley, J. C. Bridges, D. E. Brownlee, M. J. Burchell, M. Chi, M. J. Cintala, Z. R. Dai, Z. Djouadi, G. Dominguez, and 32 colleagues, Impact features on Stardust: Implications for comet 81P/Wild 2 dust, *Science*, **314**, 1716–1719, 2006.

Jenniskens, P., Optical constants of organic refractory residue, *Astron. Astrophys.*, **274**, 653–661, 1993.

Jessberger, E. K., Rocky cometary particulates: their elemental isotopic and mineralogical ingredients, *Space Sci. Rev.*, **90**, 91–97, 1999.

Joshi, U. C., K. S. Baliyan, and S. Ganesh, Polarization studies of comet C/2000 WM1 (LINEAR), *Astron. Astrophys.*, **405**, 1129–1135, 2003.

Joshi, U. C., S. Ganesh, and K. S. Baliyan, Near opposition photometry of comet C/2007 N3 (Lulin), *Mon. Not. R. Astron. Soc.*, **412**, L58–L62, 2011.

Khare, B. N., W. R. Thompson, C. Sagan, E. T. Arakawa, C. Meisse, and I. Gilmour, Optical constants of kerogen from 0.15 to 40 mm: comparison with meteoritic organics, in *Proc. Lunar Planet. Sci. Conf. 21*, 627–628, 1990.

Kiselev, N. N. and G. P. Chernova, Phase functions of polarization and brightness and the nature of cometary atmosphere particles, *Icarus*, **48**, 473–481, 1981.

Levasseur-Regourd, A. C., E. Hadamcik, and J. B. Renard, Evidence for two classes of comets from their polarimetric properties at large phase angles, *Astron. Astrophys.*, **313**, 327–333, 1996.

Mazets, E. P., R. L. Aptekar, S. V. Golenetskii, Yu. A. Guryan, A. V. Dyachkov, V. N. Ilyinskii, V. N. Panov, G. G. Petrov, A. V. Savvin, R. Z. Sagdeev, I. A. Sokolov, N. G. Khavenson, V. D. Shapiro, and V. I. Shevchenko, Comet Halley dust environment from SP-2 detector measurements, *Nature*, **321**, 276–278, 1986.

Meech, K. J. and D. C. Jewitt, Observations of Comet P/Halley at minimum phase angle, *Astrophys. J.*, **187**, 585–593, 1987.

Myers, R. V. and K. H. Nordsieck, Spectropolarimetry of comets Austin and Churyumov-Gerasimenko, *Icarus*, **58**, 431–439, 1984.

Newburn, R. L. and H. Spinrad, Spectrophotometry of 25 comets—Post-Halley updates for 17 comets plus new observations for eight additional comets, *Astron. J.*, **97**, 552–569, 1989.

Zubko, E., Interpretation of similarity in the negative polarization of comets and C-type asteroids in terms of common properties of asteroidal and cometary dust, *Earth Planets Space*, **63**, 1077–1085, 2011.

Zubko, E., Light scattering by irregularly shaped particles with sizes comparable to the wavelength, in *Light Scattering Reviews, Vol. 6: Light Scattering and Remote Sensing of Atmosphere and Surface*, edited by A. A. Kokhanovsky, pp. 39–74, Springer-Verlag, Berlin, 2012.

Zubko, E., H. Kimura, Yu. Shkuratov, K. Muinonen, T. Yamamoto, H. Okamoto, and G. Videen, Effect of absorption on light scattering by agglomerated debris particles, *J. Quant. Spectr. Rad. Trans.*, **110**, 1741–1749, 2009.

Zubko, E., D. Petrov, Ye. Grynko, Yu. Shkuratov, H. Okamoto, K. Muinonen, T. Nousiainen, H. Kimura, T. Yamamoto, and G. Videen, Validity criteria of the discrete dipole approximation, *Appl. Opt.*, **49**, 1267–1279, 2010.

Zubko, E., R. Furusho, K. Kawabata, T. Yamamoto, K. Muinonen, and G. Videen, Interpretation of photo-polarimetric observations of comet 17P/Holmes, *J. Quant. Spectr. Rad. Trans.*, **112**, 1848–1863, 2011a.

Zubko, E., G. Videen, Yu. Shkuratov, K. Muinonen, and T. Yamamoto, The Umov effect for single irregularly shaped particles with sizes comparable with wavelength, *Icarus*, **212**, 403–415, 2011b.

E. Zubko (e-mail: ezubko@rambler.ru)